Modeling of the Isobaric and Isothermal Glass Transitions of Polystyrene

Luigi Grassia,[1] Maria Giovanna Pastore Carbone,[2] Alberto D'Amore[1]

[1]*Department of Aerospace and Mechanical Engineering, The Second University of Naples, Aversa (Caserta), Italy*
[2]*Department of Materials and Production Engineering, University of Naples "Federico II," Naples, Italy*

Received 28 April 2011; accepted 28 April 2011
DOI 10.1002/app.34789
Published online 11 August 2011 in Wiley Online Library (wileyonlinelibrary.com).

ABSTRACT: The scaling law for relaxation times (τ's) recently proposed by Casalini and Roland was used in the framework of Kovacs, Aklonis, Hutchinson, and Ramos phenomenological theory. With this approach, it was shown that both the isobaric and the isothermal glass transitions of polystyrene can be reliably predicted with only two fitting parameters, namely, τ in the reference state and the fractional exponent that describes the dispersion of the α relaxation. © 2011 Wiley Periodicals, Inc. J Appl Polym Sci 122: 3752–3757, 2011

Key words: amorphous; glass transition; relaxation

BACKGROUND OF THE GLASS TRANSITION

When a material is cooled from above to below the glass-transition temperature (T_g), the resulting glass is unstable, and its density will gradually increase with time. This process toward thermodynamic equilibrium (called *structural relaxation* or, more generally, *physical aging*) occurs more rapidly at temperatures close to T_g being an activated phenomenon and manifests itself through a continuous change of a large number of properties, including but not restricted to density, enthalpy, entropy, and in turn, all of the related viscoelastic functions. The structural relaxation cannot be avoided; it occurs in all glasses, even when cooling is performed in such a way that the temperature gradients within the material are small and the resulting thermal stresses are negligible.[1]

The structural relaxation is a direct consequence of the considerably longer timescale of molecular relaxations within and below the glass-transition region compared to the experimental timescale of the applied signal. In other words, even the slowest experimentally attainable cooling rate is much too fast for the polymer chains to relax to equilibrium. The nonequilibrium structure first experiences an abrupt contraction and then undergoes a time-dependent rearrangement toward the equilibrium state. The elastic (instantaneous) contraction results from the vibration relaxations that originate in the response of the atomic bonds and whose characteristic relaxation times (τ's) are extremely short. The subsequent gradual rearrangement of the nonequilibrium structure can be followed by the monitoring of the kinetics of any structure-sensitive property changes, such as enthalpy or volume.[1]

The two principal features of structural relaxation are nonexponentiality and nonlinearity. Nonexponentiality implies that structural relaxation is subdivided into a number of processes, each characterized by its own τ. Nonlinearity, on the other hand, signifies a dependence of the structural relaxation on the direction and magnitude of the applied perturbation (i.e., temperature jump). In the literature, two main phenomelogical models have been used to predict the behavior of glass-forming materials, namely, the Kovacs, Aklonis, Hutchinson, and Ramos (KAHR) model[2,3] and the Tool–Narayanaswamy–Moynihan model.[4–6] These theories are both capable of capturing the nonlinearity and memory effect of structural relaxation. Even though the parameters of the KAHR and Tool–Narayanaswamy–Moynihan theories are strongly correlated (their use is really equivalent under isobaric conditions), KAHR theory accounts explicitly for the pressure and represents a more viable formalism to describe the pressure-volume-temperature (PVT) behavior under arbitrary temperature and/or pressure histories.[7–9] For completeness, it should be mentioned that the parameters in KAHR theory still suffer some lack of physical meaning because of the arbitrary dependence of τ on the temperature, pressure, and dimensionless volume.[7–9]

To overcome this issue, we observed that glassy materials can be obtained both by isothermal compression and isobaric cooling, which makes clear that the volume (or the pressure), along with the temperature, plays an important role in the slowing down of molecular motions.[10–13] Thus, the functional form of τ should contain both the temperature and

Correspondence to: L. Grassia (luigi.grassia@unina2.it).

the volume dependence.[10–13] Accordingly, Casalini, Roland, and coworkers[10–12] proposed the following scaling law for τ:

$$\tau(T,V) = \Im(TV^{\gamma}) \tag{1}$$

where $\Im$. is an unknown function and γ is a material-dependent constant. This scaling property has been verified for over 40 materials with different techniques, with the parameter $\gamma < 8.5$.[10–13]

Recently, Casalini, Roland, and coworkers[14,15] discussed how the scaling properties can be derived from the temperature (T) and volume (V) dependences of the entropy and, using the Avramov model,[16] derived the following expression for the $\tau(T,V)$ dependence:[14,15,17]

$$\tau(T,V) = \tau_0 \exp\left[\left(\frac{A}{TV^{\gamma}}\right)^{\phi}\right] \tag{2}$$

where τ_0, A, ϕ, and γ are constants. Equation (2) satisfies the scaling law expressed by eq. (1) and gives a good description of experimental data over a broad dynamic range.[14,15,17]

Here, the expression proposed by Casalini, Roland, and coworkers[14,15,17] is used as the functional form of τ in the KAHR model,[2,3] which predicts the volume relaxation kinetics under arbitrary pressure and temperature histories.[2,3,7–9]

The equation that describes the volume relaxation kinetics in the presence of an arbitrary temperature and pressure history reads[2,3,7–9]

$$V = V_e + V_e \int_0^{\xi} \left[-(\alpha_e - \alpha_g)\frac{dT}{d\xi'} - (k_e - k_g)\frac{dP}{d\xi'}\right] M(\xi - \xi')d\xi' \tag{3}$$

where ξ is the reduced time; the suffixes g and e indicate the glassy and equilibrium states, respectively; α is the isobaric thermal expansion coefficient; ξ' is the integration variable of the integral in the equation (3); k is the isothermal compressibility; P is the pressure; and M is the memory function, which is defined as follows:

$$M(\xi) = \exp\left[-(\xi/\tau_g)^{\beta}\right] \tag{4}$$

where τ_g is the relaxation time in the reference state, β is a fractional exponent that describes the dispersion of the α relaxation, and ξ is defined as follows:

$$\xi = \int_0^t \frac{\tau_g dt'}{\tau} \tag{5}$$

where t is the time and τ is the relaxation time. In particular, τ is expressed by eq. (2), which can be can be rewritten in terms of the isochoric fragility (m_V), which is defined as[10]

$$m_V = \left.\frac{\partial \log \tau}{\partial(T_g/T)}\right|_{T_g, V=\cos t} \tag{6}$$

From eqs. (2) and (6), it follows that parameter A is directly correlated to m_V, according to the following equation:

$$m_V = \phi\left(\frac{A}{T_g V_g^{\gamma}}\right)^{\phi}\frac{1}{\ln 10} \tag{7}$$

where T_g and V_g are the temperature and the specific volume, respectively, at the glass transition. Consequently, eq. (2) can be rewritten as

$$\ln \tau = \ln \tau_0 + \frac{m_V \ln 10}{\phi}\left(\frac{T_g V_g^{\gamma}}{TV^{\gamma}}\right)^{\phi} \tag{8}$$

At the glass transition, τ reduces to

$$\ln \tau_g = \ln \tau_0 + \frac{m_V \ln 10}{\phi} \tag{9}$$

in a way that the final expression for τ is the following:

$$\ln \tau = \ln \tau_g + \frac{m_V \ln 10}{\phi}\left[\left(\frac{T_g V_g^{\gamma}}{TV^{\gamma}}\right)^{\phi} - 1\right] \tag{10}$$

From eqs. (3), (4), (5), and (9), the constitutive equation for the specific V takes the following final expression:[18,19]

$$V = V_e + V_e \int_0^t \left[-(\alpha_e - \alpha_g)\frac{dT}{dt'} - (k_e - k_g)\frac{dP}{dt'}\right] \exp\left[-\left(\int_{t'}^{t} dt'' \Big/ \tau_g \exp\left[\frac{m_V \ln 10}{\phi}\left[\left(\frac{T_g V_g^{\gamma}}{TV^{\gamma}}\right)^{\phi} - 1\right]\right]\right)^{\beta}\right] dt' \tag{11}$$

where t'' is the integration variable of the internal integral in the equation (11).

EXPERIMENTAL

The studied polystyrene (PS) was supplied in the form of pellets by Sigma-Aldrich (Milano, Italy), with a number-average molecular weight of 130,000 and a weight-average molecular weight of 290,000 g/mol.

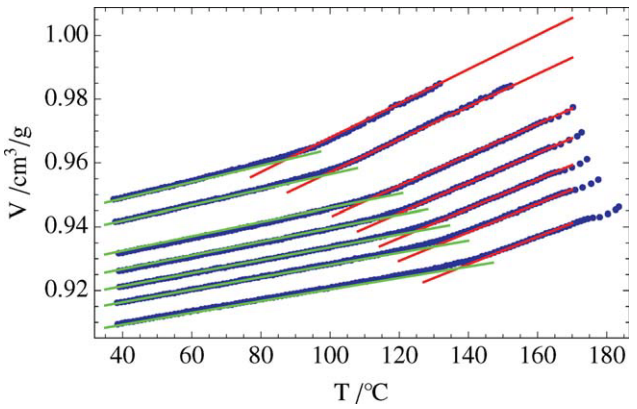

Figure 1 Isobaric PVT data (symbols) at seven different pressures, namely, 10, 30, 60, 80, 120, and 150 MPa, and at a cooling rate of 0.5°C/min. The solid lines indicate the fit of Tait's equation above (red in the online figure) and below (green in the online figure) T_g. The intersections between the two families of the curves yield the T_g's. [Color figure can be viewed in the online issue, which is available at wileyonlinelibrary.com.]

The measurements of the PVT behavior of PS were performed with a high-pressure dilatometer (GNOMIX, Boulder, CO) on the basis of the bellows technique, in which a hydrostatic pressure is applied to the sample by means of a confining fluid (mercury, in this case). It allows measurements in the pressure range 10–200 MPa and from room temperature to 400°C. The data, obtained in terms of specific volume changes as a function of the pressure and temperature, were then elaborated to obtain the absolute values of specific volume with the specific volume of the material used as a reference at a temperature of 28°C and at ambient pressure, as measured with an automatic helium picnometer (Accupyc II 1342, Micromeritics, Norcross, GA).

To evaluate the material's parameters appearing in the constitutive eq. (11), isobaric and isothermal PVT experiments were performed. The isobaric data were obtained by heating of the pressurized sample up to 160°C, aging of the sample at 160°C for 20 min, and then cooling of the sample to 25°C at a rate of 0.5°C/min. The isobaric PVT tests were carried out at seven different pressures, namely, 10, 30, 60, 80, 100, 120, and 150 MPa. Because the isobaric data below T_g were collected for an out-of-equilibrium material, k_g could not be calculated simply from isobaric experiments; hence, isothermal compression experiments were also carried out at four different temperatures below T_g (i.e., 20, 25, 29, 33, and 38°C) from 10 to 200 MPa at a pressurization rate of 13 MPa/min, with the specific purpose of evaluating k_g.

Last, to assess the model prediction capabilities, isothermal compression tests from the rubbery state to the glassy state were performed at four different temperatures, namely, 115, 130, 140, and 150°C.

RESULTS AND DISCUSSION

In what follows, we report on a procedure that, step by step, allowed us to implement eq. (11). It is shown that most of the material's functions (i.e., α_g, α_e, k_g, k_e) and the material's properties (γ, m_V and ϕ) appearing in eq. (11) could be derived directly from opportune PVT data. The remaining parameters, τ_g and β, remained as fitting parameters that could be evaluated by minimization of the sum of squared differences between the model prediction and the experimental data. Under this perspective, eq. (11) differed substantially from the original KAHR model, which requires the optimization of five parameters.[2,3,7–9]

The isobaric PVT data, obtained by the cooling of the sample from above to below T_g at 0.5°C/min, are reported in Figure 1. The measurements were performed at seven different pressures, namely, 10, 30, 60, 80, 100, 120, and 150 MPa. Tait's equation[20] $\left[V_\infty(T,P) = (a_0 + a_1 T)\left[1 - C \cdot Log\left(1 + \frac{e^{b_1 T} P}{b_0}\right)\right] \text{ with } C = 0.0894\right]$ was used here to fit the data either above or below T_g, and the results are reported in Figure 1 as red and green lines, respectively. The fitting procedure above T_g allowed us to obtain the equilibrium specific volume (V_e) at each temperature and pressure, as mentioned previously. k_e and α_e were calculated in analytical form [$k_e(T,P) = \frac{1}{V_e}\frac{\partial V_e}{\partial P}\big|_T$, $\alpha_e(T,P) = \frac{1}{V_e}\frac{\partial V_e}{\partial T}\big|_P$] from the equation of state for V_e. $\alpha_g(T,P)$ was calculated by differentiation of Tait's expression for the specific volume, which fit the data below T_g. It should be noted that the isobaric data above T_g were useful for calculating both α_e and k_e because they were equilibrium data, whereas the isobaric data below T_g could be used only to calculate the thermal

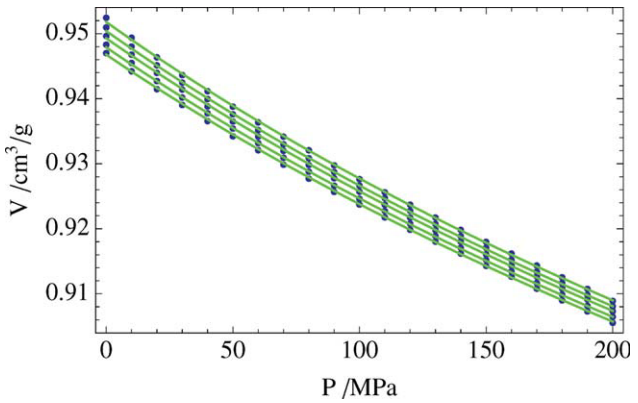

Figure 2 Isothermal PVT data (symbols) in the glassy state at five different temperatures, namely, 20, 25, 29, 33, and 38°C. The solid lines indicate the fit of Tait's equation. [Color figure can be viewed in the online issue, which is available at wileyonlinelibrary.com.]

TABLE I
Tait's Equation Parameters

	a_0 (cm^3/g)	a_1 ($cm^3\ g^{-1}\ °C^{-1}$)	b_0 (MPa)	b_1 ($°C^{-1}$)
Isobaric data above T_g	$0.9186 \pm 3.3 \times 10^{-4}$	$5.524 \times 10^{-4} \pm 2.6 \times 10^{-6}$	$1.682 \times 10^2 \pm 1.3$	$1.743 \times 10^{-3} \pm 5.5 \times 10^{-4}$
Isobaric data below T_g	$0.9418 \pm 1.2 \times 10^{-4}$	$2.661 \times 10^{-4} \pm 2.1 \times 10^{-6}$	$2.452 \times 10^2 \pm 1.2$	$1.940 \times 10^{-3} \pm 8.6 \times 10^{-5}$
Isothermal data below T_g	$0.9411 \pm 2.0 \times 10^{-4}$	$2.790 \times 10^{-4} \pm 6.9 \times 10^{-6}$	$3.373 \times 10^2 \pm 3.1$	$2.580 \times 10^{-3} \pm 3.1 \times 10^{-4}$

expansion coefficient (and k_g) because they were out-of-equilibrium data.

To calculate $k_g(T,P)$, isothermal compression experiments were performed at four different temperatures, reported in Figure 2. These isothermal PVT data were fitted with Tait's equation, as well. The Tait's model prediction is also displayed in Figure 2 as solid lines. The expression for the specific volume that came from this fitting procedure was used to analytically calculate $k_g(T,P)$.

The parameters of Tait's equations that fit the PVT isobaric data above and below T_g and the isothermal compression data below T_g are reported in Table I.

We recall that τ at different T_g's, obtained by the cooling of the sample at different pressures, should have been the same because the cooling rate was the same at each pressure. This allowed us to calculate the parameter γ because τ scaled with TV^γ; then, at T_g, the quantity $T_g V_g^\gamma$ should have been constant. In Figure 3, ln T_g is reported as function of ln V_g. The parameter γ was calculated as the slope of this curve, and the linear regression analysis gave $\gamma = 3.65 \pm 0.20$. The obtained γ value fell within the range of γ ($1.5 < \gamma < 6$) reported by Casalini and Roland[12] for other polymers.

Once γ was known, m_V could be obtained as function of γ. Indeed, the parameter γ is related to the ratio of the activation enthalpy at constant V to the activation enthalpy at constant P,[10–12] and consequently

$$\frac{m_V}{m_{P_0}} = \frac{1}{1 + \gamma\alpha_e(T_g, P_0)T_g(P_0)} \tag{12}$$

where $\alpha_e(T_g,P_0)$ and $T_g(P_0)$ are the values of the isobaric expansion coefficient and glass-transition temperature at atmospheric pressure, respectively. Furthermore, Casalini, Roland, and coworkers[10–12] showed that the isochoric and isobaric fragilities at atmospheric pressure (m_{P_0}) are linearly correlated:

$$m_{P_0} = a + bm_V \tag{13}$$

where $a = 37 \pm 3$ and $b = 0.84 \pm 0.05$. This last correlation holds true for $\tau_g = 100$ s. Here, the relaxation time at T_g (τ_g) is unknown, so m_V at T_g can be evaluated with eq. (9), as follows:

$$m_V(\tau_g) = m_V|_{\tau=100s} + \phi[\log(\tau_g) - 2]$$

m_V calculated when $\tau = 100$ s, $m_V|_{\tau=100s}$, can be obtained from eqs. (12) and (13), as follows:

$$m_V|_{\tau=100s} = \frac{a}{1 + \gamma\alpha_e(T_g, P_0)T_g(P_0) - b} \tag{14}$$

With the assumption that the product $\alpha_e T_g$ is almost constant at the glass transition, $T_g(P_0)$ was extrapolated at atmospheric pressure from the pressure dependence of T_g reported in Figure 4 (the T_g's were evaluated as the abscissa of the intersection points of

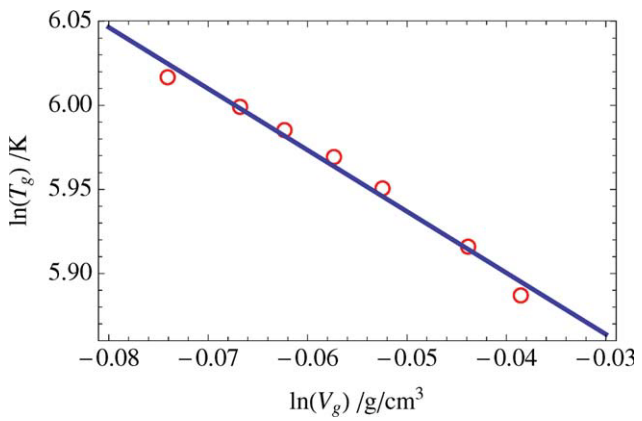

Figure 3 ln T_g versus ln V_g. The slope of the fitting straight line yields the value of g. We calculated the error bars accounting for the standard error of estimation of the Tait's equation parameters. [Color figure can be viewed in the online issue, which is available at wileyonlinelibrary.com.]

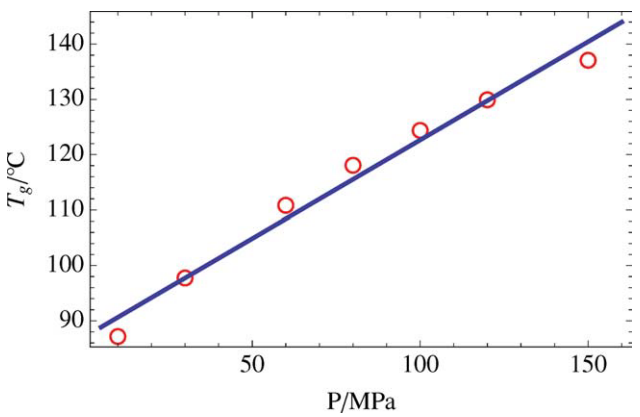

Figure 4 Pressure dependence of T_g. The solid line indicates the linear fit. The slope of the fitting line is 0.355°C/MPa. [Color figure can be viewed in the online issue, which is available at wileyonlinelibrary.com.]

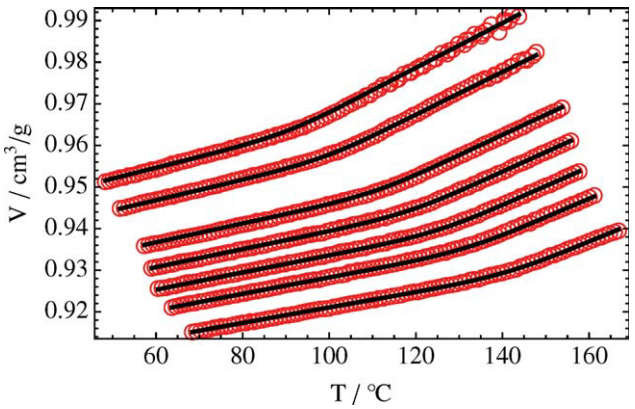

Figure 5 Isobaric PVT data for PS (symbols) and the fit based on KAHR theory modified with the Casalini and Roland scaling law for τ (solid lines). [Color figure can be viewed in the online issue, which is available at wileyonlinelibrary.com.]

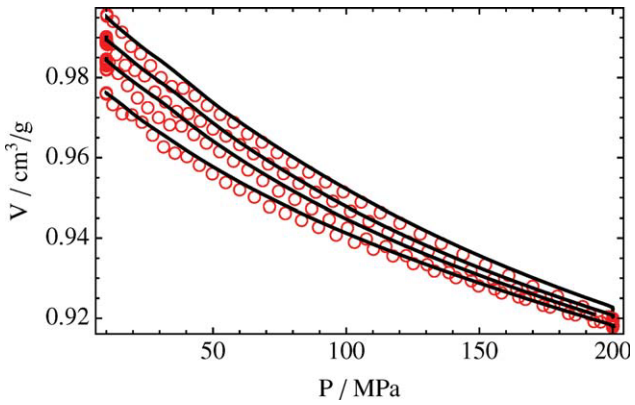

Figure 7 Glass transition obtained by isothermal compression at 115, 130, 140, and 150°C. Symbols indicated experimental data, and solid lines indicate model predictions. [Color figure can be viewed in the online issue, which is available at wileyonlinelibrary.com.]

the two families of curves that, by means of Tait's equation, fit the PVT data above and below the glass transition). $\alpha_e(T_g,P_0)$ was calculated with Tait's equation, which fit the volumetric data above T_g. From eq. (14), $m_V|_{\tau=100s}$ was 40.6 ± 7.

Finally, with the correlation between ϕ and γ[17]

$$\phi = \frac{20.8 \pm 0.9}{1+\gamma} \tag{15}$$

we found $\phi = 4.47 \pm 0.40$.

The parameters τ_g and β were evaluated by minimization of the sum of the square differences between the modeling predictions and the experimental results in terms of the specific volume obtained by the cooling of the sample from above to below T_g (i.e., by the fitting of the experimental PVT data reported in Fig. 1). The values of ln τ_g and β that minimized the sum of square differences were 7.15 and 0.33, respectively.

The results of the fitting procedure are displayed in Figures 5 and 6 in terms of the specific volume and its temperature derivative [$\partial V/\partial T$], where the experimental data are displayed with symbols and the modeling predictions are displayed as solid lines. The proposed modeling approach was able to predict both the asymptotic behavior, deep in the glassy and rubbery states, and the volume relaxation kinetics by means of a single set of theory parameters that remained fixed once and for all.

The model was then used to predict the volume response of PS in its pressure-induced glass transition, as revealed by isothermal compression at four different temperatures (i.e., 115, 130, 140, and 150°C). The samples were first heated isobarically at 10 MPa up to 160°C, aged at 160°C and 10 MPa for 20 min, cooled at 10 MPa to the temperature of interest, and finally, isothermally compressed up to 200 MPa. For the sake of clarity, only this last step is reported in Figure 7, where the experimental results are displayed as symbols and the model prediction are displayed as solid lines. The agreement between the experimental results and the model predictions was quite good, and consequently, the proposed modeling approach represents a reliable way to predict the volumetric behavior of glass-forming systems in the region of α relaxation.

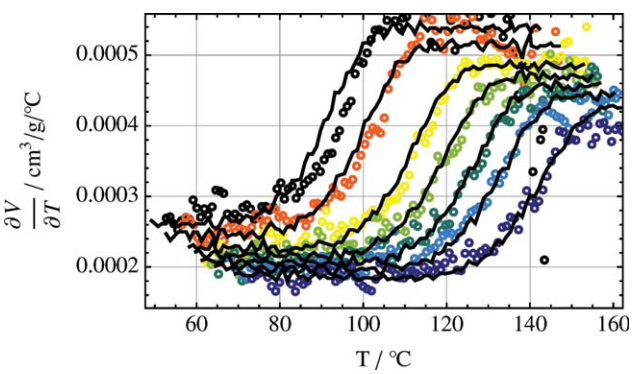

Figure 6 Temperature derivative of the isobaric volumetric data (symbols) and the modeling predictions (solid lines). The fitting procedure was implemented on the absolute values of the specific volume. This figure highlights the capability of the model to predict the structural relaxation kinetics. [Color figure can be viewed in the online issue, which is available at wileyonlinelibrary.com.]

CONCLUSIONS

The scaling law for τ, recently proposed by Casalini and Roland, was implemented in a modified KAHR model to predict the volume relaxation kinetics. With this approach, the model contained only two fitting parameters (i.e., τ_g and β, which describe the dispersion of the α relaxation), instead of the five

parameters of classical KAHR theory. The two model parameters were calculated by the fitting of the isobaric PVT data, obtained by the cooling of the sample from above to below T_g, and fixed once and for all. The prediction capability of the model was then tested by the comparison of the predictions with the results in terms of PS density evolution obtained in the pressure-induced glass transition. The agreement between the experimental results and the model predictions was quite good, and consequently, the proposed modeling approach represents a reliable way to predict the volumetric behavior of glassy systems obtained isobarically and isothermally in the region of α relaxation.

References

1. Han, Y.; D'Amore, A.; Nicolais, L. J Mater Sci 1999, 34, 1899.
2. Kovacs, A. J.; Aklonis, J. J.; Hutchinson, J. M.; Ramos, A. R. J Polym Sci Part B: Polym Phys 1979, 17, 1097.
3. Ramos, A. R.; Kovacs, A. J.; O'Reilly, J. M.; Tribone, J. J. J Polym Sci Part B: Polym Phys 1988, 26, 501.
4. Tool, A. Q. J Am Ceram Soc 1946, 29, 240.
5. Narayanaswamy, O. S. J Am Ceram Soc 1971, 54, 491.
6. DeBolt, M. A.; Easteal, A. J.; Macedo, P. B. C.; Moynihan, T. J Am Ceram Soc 1976, 59, 16.
7. Grassia, L.; D'Amore, A. Phys Rev E 2006, 74, 021504.
8. Grassia, L; D'Amore, A. J Polym Sci Part B: Polym Phys 2009, 47, 724.
9. Grassia, L; D'Amore, A. J Rheol 2009, 53, 339.
10. Roland, C. M.; Paluch, M.; Hensel-Bielowka, S.; Casalini, R. Rep Prog Phys 2005, 68, 1405.
11. Casalini, R.; Roland, C. M. Phys Rev E 2004, 69, 062501.
12. Casalini, R.; Roland, C. M. Phys Rev E 2005, 72, 031503.
13. Huang, D.; Colucci, D. M.; McKenna, G. B. J Chem Phys 2002, 116, 3925.
14. Casalini, R.; Mohanty, U.; Roland, C. M. J Chem Phys 2006, 125, 014505.
15. Casalini, R.; Roland, C. M. Philos Mag 2007, 87, 459.
16. Avramov, I. J Non-Cryst Solids 2000, 262, 258.
17. Casalini, R.; Roland, C. M. J Non-Cryst Solids 2007, 353, 3936.
18. Grassia, L.; D'Amore, A. J Non-Crystalline Solids 2011, 357, 414.
19. Grassia, L.; D'Amore, A. AIP Conf Proceed 2010, 1255, 417.
20. Tait, P. G. The Voyage of H. M. S. Challenger; Her Majesty's Stationary Office: London, 1888; Vol. 2.